Available online at http://www.journalijdr.com

IJDR

ISSN: 2230-9926

International Journal of Development Research
Vol. 12, Issue, 02, pp. 54029-54034, February, 2022
https://doi.org/10.37118/ijdr.23985.02.2022

RESEARCH ARTICLE

OPEN ACCESS

EVALUATION OF HEAT TRANSFER COEFFICIENTS BY CFD AND RESPONSE SURFACE TECHNIQUES

Yanne Novais Kyriakidis*, Danylo de Oliveira Silva and Luiz Gustavo Martins Vieira

Federal University of Uberlândia, School of Chemical Engineering, 1K – Campus Sta. Mônica

ARTICLE INFO

Article History:
Received 11th February, 2022
Received in revised form
16th February, 2022
Accepted 19th February, 2022
Published online 20th February, 2022

Key Words:
Thermal Convection, Flow Regime, Physicochemical Properties, Transport Equations.

Corresponding author:
Yanne Novais Kyriakidis

ABSTRACT

Heat Transfer Coefficients are extremely important for design and control of thermal processes involving the convection mechanism. Experimental evaluation of the film coefficients is not simple because such parameters depend on the system geometry, flow regime and physicochemical properties of the fluid. Thus, an interesting alternative for estimating the convective heat transfer coefficient is to apply CFD techniques to solve the transport equations numerically. Therefore, this study aimed to apply the CFD techniques to evaluate the *Nusselt Number* in a spherical geometry under different flow conditions, compare the values obtained with those from the literature and correlate them according to the *Reynolds* and *Prandtl Numbers* through the *Response Surface Methodology*. The CFD techniques combined with the *Response Surface Methodology* were feasible and showed satisfactory results to predict the convective *Heat Transfer Coefficients*.

Citation: ***Yanne Novais Kyriakidis, Danylo de Oliveira Silva and Luiz Gustavo Martins Vieira.*** "Evaluation of heat transfer coefficients by cfd and response surface techniques*", International Journal of Development Research*, 12, (02), 54029-54034.

INTRODUCTION

All energy forms are important to the professional work of engineers. However, when it comes to Transport Phenomena, it is necessary to give attention to heat transfer (by thermal energy), that occurs through three mechanisms: conduction, convection and radiation. Among the mechanisms of heat transfer, the convective heat transport requires special treatment because of the inherent link between this phenomenon and the momentum transport [1, 2, 3, 4, 5, 6]. The heat convection is only possible due to thermal gradients within a fluid and by the flow (forced or natural) of the fluid through the system. In theory, it is possible to calculate all thermal gradients or heat rates in a fluid from the perspective of Transport Phenomena [7], through joint solution of the *Thermal Energy Equation* with the *Equation of Motion* and the *Continuity Equation* (supported by a *Equation of State* and correlations for describing other physical properties depending on temperature and pressure). However, in practice, the above-mentioned solution is not trivial due to the mathematical and computational complexity required by the phenomenon [8]. Thus, a much-used alternative to describe the effects of convection is *Newton's Law of Cooling* (Equation 1). A relatively simple algebraic equation that attempts to correlate the heat rate transported with physical quantities of immediate perception (area available for transfer and thermal gradient) is the basis of *Newton's Law of Cooling*. These quantities are related by a proportionality constant (h), called *Heat Transfer Coefficient* [9].

$$Q = h\ A\ \left(T - T_{\infty}\right) \tag{1}$$

In general, the knowledge of the *Heat Transfer Coefficient* (h) is essential for the design of equipment – evaporators, heat exchangers, reactors, distillers, boilers, fluidized bed etc. – and the lack of that hampers any decision-making [10, 11, 12, 13, 14]. *Heat Transfer Coefficients* are not quantities only regarding the properties of matter, but also depend on the characteristics of the flow field [15, 16, 17, 18] and geometry of the system under analysis [19, 20]. Thus, prior to project thermal equipment, it is a necessary precondition to know the *Heat Transfer Coefficients* or a way to obtain them [21]. Traditionally, *Heat Transfer Coefficients* are determined experimentally, requiring specific instrumentation, a reasonable financial investment and labor empirical procedures [22, 23, 24]. Nowadays, due to advances in the computational field [25] it is possible to evaluate the properties of flows through the transport equations [26] in software that make use of numerical computational techniques called *Computational Fluid Dynamics* (CFD). Thereby, this paper aimed to use the CFD techniques to verify the feasibility of estimating numerically the average *Heat Transfer Coefficients* in spherical surfaces, such that this methodology could be generalized and also be applied to other geometries, including complex ones (paraboloids, ellipsoids, saddles, logs, cones, frustums etc.). Besides that, to obtain appropriate correlations for the assessment of *Heat Transfer Coefficients*, the *Response Surface Methodology* (RSM) was also accomplished.

MATERIALS AND METHODS

In order to verify the feasibility of the CFD techniques for the numerical evaluation of *Heat Transfer Coefficients*, it was designed a "wind tunnel" equipped with a spherical rigid body (specimen), inserted into the center of a circular cross section duct. Figure 1 depicts the geometrical dimensions and the arrangement of the elements in the wind tunnel.

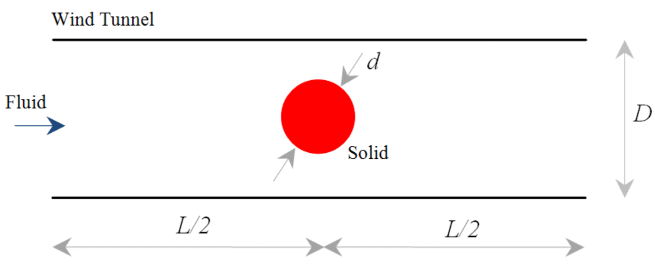

Figure 1. Schematic view of the wind tunnel with *d*, *D* and *L* equal to 0.02, 0.20 and 0.40 m, respectively

Figure 2 shows details of the mesh generated for the wind tunnel in the GAMBIT® 2.3.16 software. The computational mesh used in this study was three-dimensional, refined close to solid surfaces (specimen and the duct walls), with approximately $2x10^5$ tetrahedral cells. The grid size was determined by ensuring that it was sufficiently fine to achieve grid independence [27], in which this amount of cells showed no more change in some property of the system (Figure 3), for example, the heat flux (q) transferred from the sphere to the fluid.

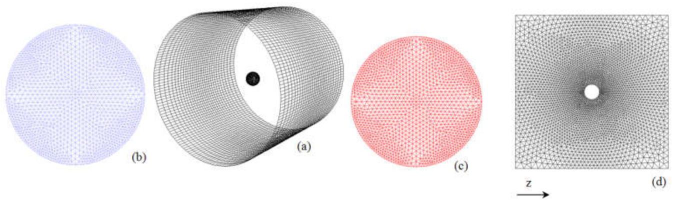

Figure 2. Wind tunnel geometry illustrating the details of the mesh structure: (a) wind tunnel walls, (b) entry section, (c) output section and (d) cross section

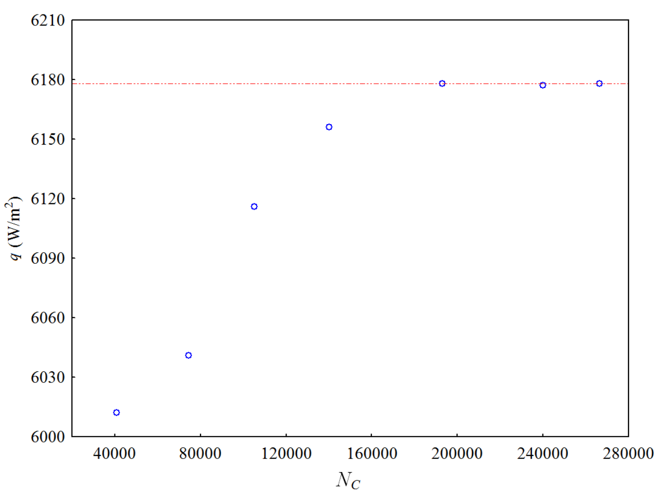

Figure 3. Grid independence test to determine the number of computational cells

The CFD simulations have been performed according to a *Full Factorial Design* [28]. For this numerical study, *Reynolds Number* (*Re*) and *Prandtl Number* (*Pr*) were the independent variables that have been manipulated to obtain *Nusselt Number* (Nu) (response or dependent variable), whose expressions are represented by Equations 2, 3 and 4, respectively.

$$Re = \frac{\rho_\infty v_\infty d}{u_\infty} \tag{2}$$

$$Pr = \frac{\mu_\infty c_{p\infty}}{k_\infty} \tag{3}$$

$$Nu = \frac{hd}{k_\infty} \tag{4}$$

It is worth mentioning that the characteristic dimension for calculating the *Reynolds Number* (*Re*) is the sphere diameter (*d*) inside the wind tunnel. In turn, the physical properties of the fluid needed to determine the dimensionless numbers (*Re*, *Pr*) have been evaluated in the fluid approximation temperature (T_∞). Each one of these numbers was studied at 3 different levels using a *Full Factorial Design* (3^2), shown in Table 1.

Regarding *Prandtl Number*, the variation of this dimensionless quantity was only possible by using different fluids (air, kerosene and ethylene glycol). Unlike *Reynolds Number*, the variation of *Prandtl Number* was not equally spaced (manipulated) because it is intrinsically dependent on the physicochemical nature of the fluid; so, it is not possible, for the user, to place it in specific intermediate levels. Under the conditions presented in Table 1, Pr and Re factors have been coded (Equations 4 and 5) aiming at the posterior multiple regression [29], in order to evaluate possible existing effects (linear, quadratic and interaction) on the *Heat Transfer Coefficients*. In this case, the *Prandtl Numbers* of air, kerosene and ethylene glycol have been coded to -1.0000, -0.6347 and +1.0000, respectively. The *Reynolds Number* of 100, 5050 and 10000 have been coded to -1, 0 and +1, respectively. Equations 5 and 6 represent the respective coding equations for *Reynolds* and *Prandtl Numbers*.

$$X_1 = \frac{Pr - 75.37}{74.63} \tag{5}$$

$$X_2 = \frac{Re - 5050}{4950} \tag{6}$$

For each one of the operating conditions of the Design Matrix (Table 1), simulations have been performed in the CFD package FLUENT® 14.0 for the system shown in Figure 1. The simulations were performed on transient regime; the turbulence model, the pressure-velocity coupling algorithm and the interpolation scheme used in the simulations were LES (Large Edge Simulation [30]), SIMPLE (Semi Implicit Linked Equations [31]) and QUICK (Quadratic Upstream Interpolation for Convective Kinematics [32]), respectively. Table 2 shows the other necessary numeric-operating conditions for CFD simulations. Having completed each one of the *N* simulations (Table 1), it is known that the *i* computational cells along with the solid (A_i dimension) have transferred the respective heat rate (Q_i) to the adjacent fluid. These quantities were intrinsically related by *Newton's Law of Cooling*, in the form of Equation 7.

$$h_i = \frac{Q_i}{A_i\left(T_S - T_\infty^i\right)} \tag{7}$$

Thus, the average value of *Heat Transfer Coefficient* (*h*) could be evaluated by integrating Equation 7 over the entire surface of the specimen, according to Equation 8. This task has been performed with the use of the *Surface Integrals Function* contained in package FLUENT® 14.0.

$$h = \frac{\int_0^\pi \left\{ \int_0^{2\pi} (h_i) \left[\left(\frac{d}{2} \right)^2 sen\theta \right] d\varphi \right\} d\theta}{\int_0^\pi \int_0^{2\pi} \left[\left(\frac{d}{2} \right)^2 sen\theta \right] d\varphi d\theta} \tag{8}$$

Table 1. Experimental Design to obtain the Heat Transfer Coefficients

N	Fluid (Pr)	Re	N	Fluid (Pr)	Re	N	Fluid (Pr)	Re
01	Air (0.71)	100	04	Kerosene (28)	100	07	Ethylene glycol (150)	100
02	Air (0.71)	5050	05	Kerosene (28)	5050	08	Ethylene glycol (150)	5050
03	Air (0.71)	10000	06	Kerosene (28)	100000	09	Ethylene glycol (150)	10000

Table 2. Numerical and operating conditions used for the simulations

Fluid	air, kerosene and ethylene glycol
Fluid approximation temperature (T_∞)	298 K
Solid surface temperature (T_S)	398 K
Time step	$1x10^{-6}$ s
Convergence criteria	$1x10^{-4}$
Wind tunnel outlet pressure	95245 Pa (Uberlândia, Brazil)

With the values generated by the simulations (*Surface Integrals Function*), it was possible to apply on them the *Response Surface Methodology* [33], in order to obtain the *Regression Equation* to quantify the effects exerted by Reynolds and Prandtl numbers on Nusselt number. A general Regression Equation is given by Equation (9), with the following parameters to be estimated: an independent or average coefficient (β), the linear interaction coefficient (b_1 and b_2), quadratic coupling coefficients (B_{11}, B_{22}) and a cross-product coefficient (B_{12}=B_{21}).

$$h = \beta + \begin{pmatrix} b_1 & b_2 \end{pmatrix}\begin{pmatrix} X_1 \\ X_2 \end{pmatrix} + \begin{pmatrix} X_1 & X_2 \end{pmatrix}\begin{pmatrix} B_{11} & \frac{B_{12}}{2} \\ \frac{B_{21}}{2} & B_{22} \end{pmatrix}\begin{pmatrix} X_1 \\ X_2 \end{pmatrix} \tag{9}$$

Finally, it is noteworthy that prior to obtaining the effects of the Equation (9), the mean values of *Nusselt Numbers* obtained by this methodology (CFD) were compared with those predicted by the *Whitaker Correlation* [34], represented by Equation (10), and by the *Ahmed-Yovanovich Correlation* [35], given by Equation (11).

$$Nu = 2 + \left(0.4\,Re^{1/2} + 0.06\,Re^{2/3}\right)Pr^{2/5}\left(\frac{\mu_\infty}{\mu_S}\right)^{1/4} \tag{10}$$

$$Nu = 2 + 0.775\frac{Re^{1/2}\,Pr^{1/3}}{\left[\frac{2}{\left(1+Re^{1.25}\right)^{1/6}}+1\right]^{1/2}\left\{1+\frac{1}{\left[\frac{2}{\left(1+Re^{1.25}\right)^{1/6}}+1\right]^{3}Pr}\right\}^{1/6}} \tag{11}$$

The *Whitaker Correlation*, with an empirical approach, represents a classic of literature to estimate the average *Nusselt Number* in spherical geometries subjected to gas flows. In turn, the *Ahmed-Yovanovich Correlation* is based on the approximate analytic solution from the linearization of the *Energy Equation*, and it can be used for heat transfer of spheres to liquids and gases.

RESULTS

In order to verify the CFD proposed methodology, some preliminary simulations have been carried out using air and water (in addition to those already given by the Design Matrix – Table 1). The mean values of *Nusselt Numbers* obtained through CFD simulations were compared to those given by the *Whitaker Correlation* (applicable only to gas flows, past single spheres) and the *Ahmed-Yovanovich Correlation* (applicable to gas or liquid flows, past spheres). Figure 4 and Figure 5 present these results.

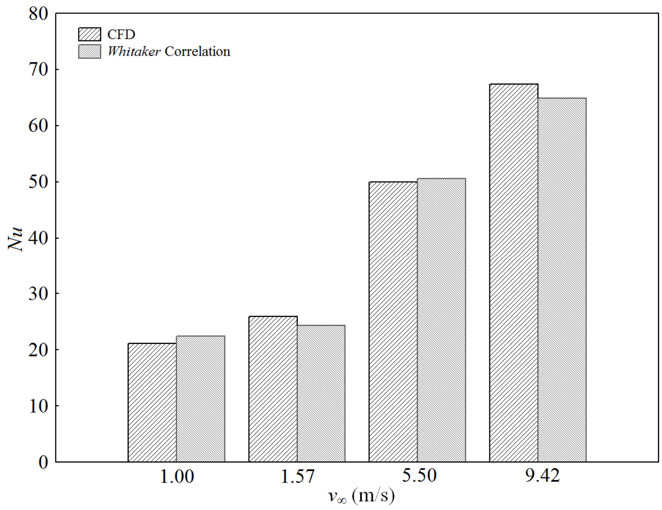

Figure 4. Mean values of *Nusselt Number* estimated by CFD techniques and by the *Whitaker Correlation* for air at 298 K

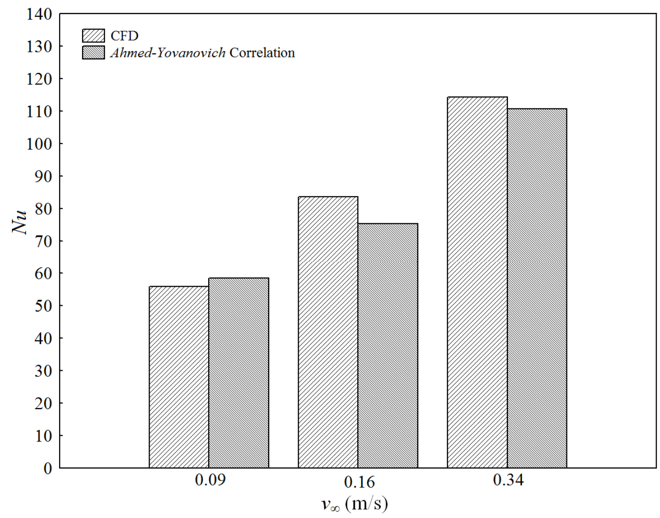

Figure 5. Mean values of *Nusselt Number* estimated by CFD techniques and by the *Ahmed-Yovanovich Correlation* for water at 298 K

Figures 4 and 5 show that the CFD techniques were satisfactory because they have reasonably predicted the mean values of *Nusselt Numbers* for the two systems. There was a mean difference of 2.33% compared to the *Whitaker Correlation* and a mean difference of 5.23% with respect to the *Ahmed-Yovanovich Correlation*. Although *Whitaker* and *Ahmed-Yovanovich Correlations* did not meet the confidence intervals of the *Nusselt Numbers* values predicted by their correlations, it is believed that the CFD techniques have been satisfactory and statistically equivalent. Therefore, the methodology proposed in this study could be applied to other cooling processes, using different fluids, including those of the Design Matrix (kerosene and ethylene glycol). Figures 6 and 7 show the velocity profile and the thermal distributions for the different flow regimes.

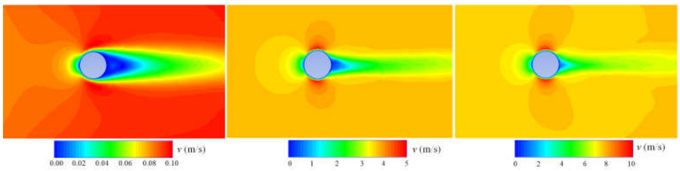

Figure 6. Air velocity profiles (*Pr* = 0.74) around the sphere for different flow regimes: (a) *Re* = 100, (b) *Re* = 5050 and (c) *Re* = 10000

According to Figure 6, it can be noticed that the sphere, due to its spatial location, has been subjected to a uniform velocity distribution, indicating that the ratio of the sphere diameter and the wind tunnel diameter was well chosen and also appropriate for the purposes of this study (d/D = 0.10). However, close to the sphere, it can be seen a strong interaction between the fluid and the solid surface. At first, there was the formation of a boundary layer prior to the solid structure, whereas after that, it has produced a von Karman vortex street. This fluid dynamic behavior has indicated the real need of using a turbulence model, as the Large Edge Simulation (LES), for the physical-mathematical description of the flow.

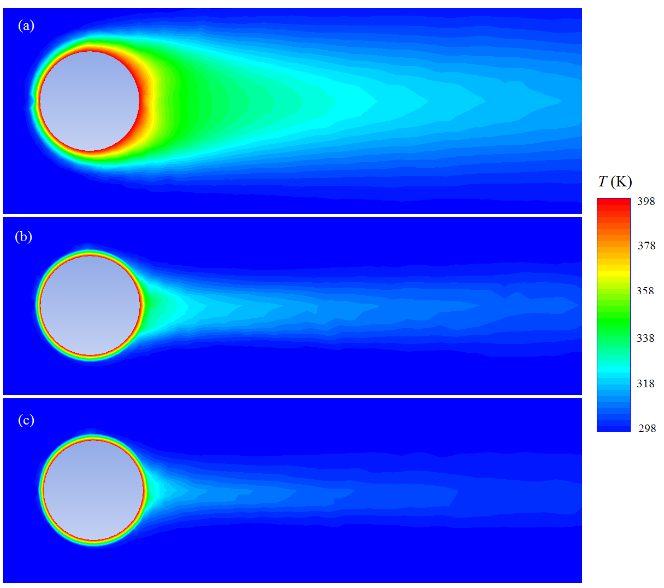

Figure 7. Air thermal distribution (*Pr* = 0.71) around the sphere for different flow regimes: (a) *Re* = 100, (b) *Re* = 5050 and (c) *Re* = 10000

Analogously to the velocity profiles, it was also possible to observe the consistency for the temperature distribution throughout the fluid flow. According to Figure 7, immediately before the sphere, the cold fluid suffered a sudden heating, because in this region heat transfer is always the most effective because of the existence of the higher thermal gradients. With the advance of the flow around the sphere, fluid temperatures tended to increase because of the effects of turbulence that cause mixing of high temperature fluid parcels with the low temperature ones. Consequently, after a reasonable distance ahead of the sphere, it was achieved a uniform temperature, close to that of the fluid approximation (T_∞). As mentioned before, based on the methodology described in this paper for the Design Matrix showed in Table 1, it was possible to estimate the *Nusselt Number* for each one of the numerical experiments by means of the Surface Integrals function, after the CFD simulations. Figure 8 presents these simulated values. According to the information of Figure 8, both the flow regime (directly related to the *Reynolds Number*) and the type of cooling fluid (directly related to the *Prandtl Number*) exerted significant influences on the *Nusselt Numbers*.

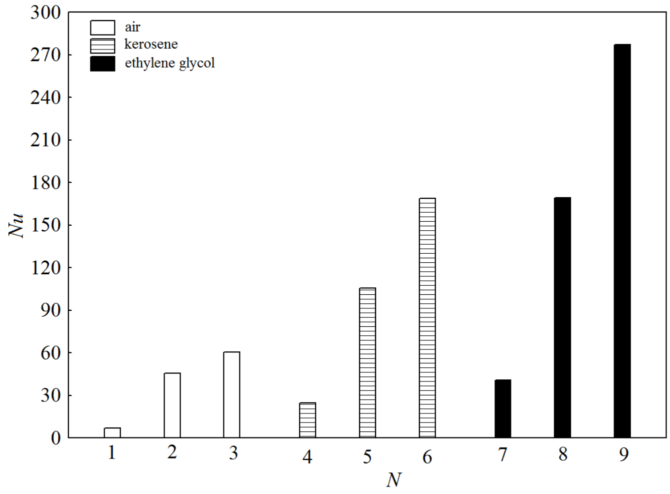

Figure 8. Nusselt numbers obtained via CFD from the combination of *Prandtl* and *Reynolds Numbers* of the Design Matrix (Table 1)

In the same flow regime, the cooling using liquid provided a substantial increase in heat transfer rate in comparison to that using gas. Only by way of example, *Heat Transfer Coefficient* increased by 17 times when air was replaced by kerosene and 50 times when the replacement of this gas by ethylene was performed. The increase in heat transfer to the liquid was also evident in the thermal distributions ahead of the sphere, as illustrated by the fluid dynamic simulations of Figure 9.

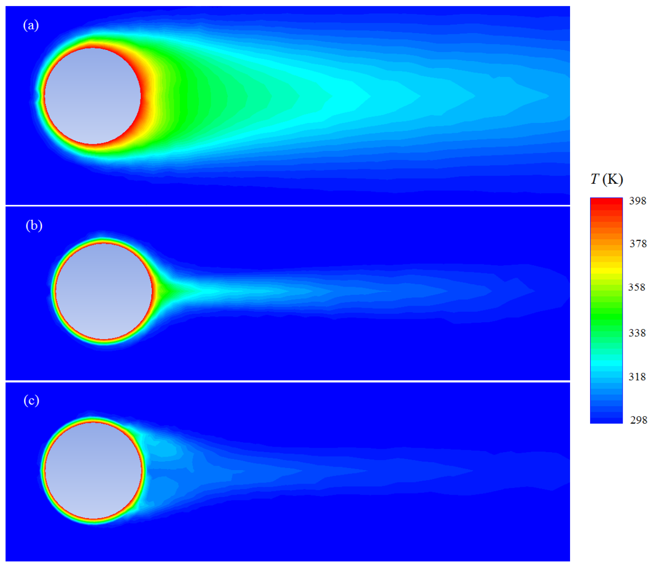

Figure 9. Thermal distribution around the sphere for different fluids at *Re* = 100: (a) air, (b) kerosene and (c) ethylene glycol

The CFD simulations showed a smaller spread of the temperature ahead of the specimen for the liquids. The lower thermal scattering usually occurs because the kinematic viscosity (ν) of good refrigerants is predominant over its thermal diffusivity (α), reflecting directly on the magnitude of the *Prandtl Number* (ν/α). Therefore, among the fluids analyzed, ethylene glycol showed a better performance compared to kerosene and this was better than air. In order to quantify the effect of each independent variable (*Re*, *Pr*) over the studied response (*Nu*), the Response Surface Methodology has been applied to the simulated set of information to obtain the respective *Regression Equation*. Table 3 presents the effects with a significance level (p-level) equal to or less than 5%. Non-significant effects (p-level > 5%) have received the value zero. Even after excluding the non-significant effects, the Regression Equation still kept a reliability or variance (R^2) of 98.13%. The residual analyses of the regression show that the residuals were independently and identically distributed according to a normal distribution with mean zero and fixed variance.

Table 3. Regression summary for dependent variables: *Pr* and *Re*

Response (*Nu*) [R^2 = 0.9813]		
Coded variables	Effects	p-level (%)
β	165.6	0.0917
b_1	62.4	0.0883
b_2	80.9	0.0362
B_{11}	-65.7	3.8600
B_{22}	0.0	46.000
B_{12}	40.4	0.0752

DISCUSSION

According to the Regression Results (Table 3), the *Prandtl Number* (*Pr*) and the *Reynolds Number* (*Re*) have directly affected the value of the *Nusselt Number*. Despite the importance of both, it is noteworthy that the flow regime (*Reynolds*) has shown prominent effect on the heat transfer, due to the comparison of magnitude between the linear effects of *Pr* and *Re* (62.4 and 80.9, respectively). In addition, it became clear the reason why the *Heat Transfer Coefficients* of ethylene glycol (higher *Prandtl*) were, on average, 50 times higher than those obtained with air. This was due to the strong effect of the *Prandtl* also exerted on the *Nusselt*. The same reason applies to kerosene, which presented *Heat Transfer Coefficients* about 17 times greater than air. With respect to the quadratic effects, only the *Prandtl Number* was significant for heat transfer (B_{11} = -65.7), since the effect of quadratic interaction of *Reynolds Number* was zero (B_{22} = 0). Furthermore, there was also a cross-product effect between the factors under study (B_{12} = 40.4). From the results of Figure 8, it was possible to propose a new correlation to describe adequately the Nusselt number as a function of Reynolds and Prandtl numbers (Equation 12). It is noteworthy that Equation (12) followed the shape commonly presented in the literature [36, 37, 38]. The ranges of validity of this Correlation are $0.71 \leq Pr \leq 150.00$ and $100 \leq Re \leq 10000$.

$$Nu = \left(0.47 \pm 0.03\right) Re^{0.28\pm0.02}\, Pr^{0.54\pm0.07}\ (R^2=0.9928) \qquad (12)$$

With all of the above discussions, it can be stated that the *Computational Fluid Dynamics Techniques* (CFD) were able to predict with satisfactory reliability the *Nusselt Numbers*. This fact represented a breakthrough for the field of convection heat transfer, because this methodology can be generalized to other geometries, including complex, for which experimental determination of *Heat Transfer Coefficients* can be costly, inaccurate or even impossible by the traditional methods. In addition, the obtained Correlation by Response Surface Methodology and CFD techniques (Equation 12) is useful because it comprises, in the same structure, a wide operating range for *Re* and *Pr*, as well as a general expression that can be satisfactorily applied to gases and liquids. *Heat Transfer Coefficients* for spherical geometries have been estimated using *Computational Fluid Dynamic Techniques* (CFD). *Nusselt Numbers* numerically estimated by CFD have been compared with values from classical empirical correlations of *Whitaker* (1972) and *Ahmed-Yovanovich* (1994), with a mean relative deviation of only 2.33% and 5.23%, respectively. A Full Factorial Design showed that both the *Reynolds Number* and the *Prandtl Number* have directly affected the heat transfer. However, in the case of heat transfer in spherical geometry, the results have indicated that the effect of flow regime (intrinsically related to *Reynolds Number*) was more significant than the nature of the fluid (related to *Prandtl Number*). It was possible to conclude that, in the same flow regime, cooling with ethylene glycol (liquid) has provided heat transfer coefficients about 50 times greater than when using air. From the numerical methodology described in this study, it was possible to propose a new Correlation more general than that of *Whitaker* (applicable only to gases) and mathematically simpler than that of *Ahmed-Yovanovich* (applicable to liquids and gases). Finally, it was concluded that the CFD techniques can be probably extended to other geometries (including complex), allowing engineers to obtain "numerical" correlations according to the geometry of interest and the used fluids.

Acknowledgment

The authors are thankful to the Brazilian Research Agencies Conselho Nacional de Desenvolvimento Científico e Tecnológico (Proj.422749/2013-7) and Fundação de Amparo à Pesquisa do Estado de Minas Gerais (CRA/APQ-01931/13 and APQ-00716-14) for financial support, and to the Separating and Renewable Energy Laboratory (LASER) of Chemical Engineering School of Federal University of Uberlândia (FEQUI/UFU).

SYMBOLS

A – area available for heat transfer in convection (m^2)
A_i – area available for heat transfer in convection in the computational cell i (m^2)
b_1 - linear interaction coefficient for *Prandtl Number* (-)
b_2 - linear interaction coefficient for *Reynolds Number* (-)
B_{11} - quadratic coupling coefficient for *Prandtl Number* (-)
B_{12} - cross-product coefficient between *Prandtl* and *Reynolds Numbers* (-)
B_{22} - quadratic coupling coefficient for *Reynolds Number* (-)
$c_{p\infty}$ – estimated specific heat of the fluid at T_∞ (J/kg)
d – massive sphere diameter (m)
D – wind tunnel diameter (m)
h – average *Heat Transfer Coefficient* [W/(m^{2}K)]
h_i – *Heat Transfer Coefficient* for the computational cell i [W/(m^{2}K)]
k_∞ – thermal conductivity of the fluid estimated at T_∞ [W/(m.K)]
φ - zenith angle (rad)
μ_∞ – dynamic viscosity of the fluid estimated at T_∞ [kg/(m.s)]
L – wind tunnel length (m)
N – sequence of the CFD simulations
N_C – number of computational cells
Nu – *Nusselt Number*
Pr – *Prandtl Number*
q – convection heat flux (W/m^2)
Q – rate of heat transfer in convection (W)
Q_i – rate of heat transfer of the computational cell i transported in convection (W)
Re – *Reynolds Number*
v_∞ – fluid approximation velocity (m/s)
T – fluid temperature (K)
T_S – solid temperature (K)
T_∞ – fluid approximation temperature (K)
X_1 – coded variable related to *Prandtl Number*
X_2 – coded variable related to *Reynolds Number*
β – independent or average coefficient of the *Response Surface Equation* [W/(m^{2}K)]
θ - azimuthal angle (rad)
μ_S – dynamic viscosity of the fluid estimated at T_S [kg/(m.s)]
ρ_∞ – density of the fluid estimated at T_∞ (kg/m^3)

REFERENCES

Ahmed, G.R., Yovanovich, M.M. (1996) Experimental study of forced convection from isothermal circular and square cylinders and toroids, Journal of Heat Transfer 119, pp 70-79, DOI: 10.1115/1.2824102

Azmi, W.H., Sharma, K.V., Sarma, P.K., Mamat, R., Anuar, S. (2014) Numerical validation of experimental heat transfer coefficient with SiO_2 nanofluid flowing in a tube with twisted tape inserts, Applied Thermal Engineering 73, pp 296-306, DOI: http://dx.doi.org/10.1016/ j.applthermaleng.2014.07.060

Bhapkar, U.S., Mohanan, S., Agrawal, A., Srivastava, A. (2014) Interferometry based whole-field heat transfer measurements of an impinging turbulent synthetic jet, International

Communications in Heat and Mass Transfer 58, pp 118-124, DOI: http://dx.doi.org/10.1016/ j.icheatmasstransfer.2014.08.040

Bird, R.B., Stewart, W.E., Lightfoot, E.N. (2007) Transport Phenomena, second ed., John Wiley & Sons, New York.

Blaszczuk, A., Nowak, W. (2014) Bed-to-wall heat transfer coefficient in a supercritical CFB boiler at different bed particle sizes, International Communications in Heat and Mass Transfer 79, pp 736-749, DOI: http://dx.doi.org/10.1016/ j.ijheatmasstransfer. 2014.08.080

Box, M.J., Hunter, W.G., Hunter, J.S. (1978) Statistics for experiments: an introduction to design, data analysis and model building. first ed., John Wiley and Sons, New York.

Bozzoli, F., Cattani, L., Rainieri, S., Pagliarini, G. (2014) Estimation of local heat transfer coefficient in coiled tuber under inverse heat conduction problem approach, Experimental Thermal and Fluid Science 59, pp 246-256, DOI: http://dx.doi.org/ 10.1016/j.exp thermflusci.2013.11.024

Churchill, S.W. (1977) M. Bernstein, *Journal Heat Transfer.* 99, pp 300.

Dahikar, S.K., Joshi, J.B., Shah, M.S., Kalsi, A.S., RamaPrasad, C.S., Shukla, D.S. (2010) Experimental and computational fluid dynamic study of reacting gas jet in liquid: Flow pattern and heat transfer, Chemical Engineering Science 65, pp 827-849, DOI:10.1016/j.ces.2009.09.035

Damasceno, J.J.R., Vieira, L.G.M., Rocha, S.M.S., AGUIAR, M.L. (2009) Fluid Dynamics study of the influence position on the feed in fabric filters, Computer-Aided Chemical Engineering 27, pp 1083-1088, DOI: 10.1016/S1570-7946(09)70401-8

Fang, X., Zhou, Z., Wang, H. (2015) Heat transfer correlation for saturated flow boiling of water, Applied Thermal Engineering 76, pp 147-156, DOI: http://dx.doi.org/10.1016/ j.applthermaleng.2014.11.024

Hilpert, R. (1933) Forsch Geb. Ingenieurwes. 4, pp 215.

Incropera, F.P., DeWitt, D.P., Bergman, T.L., Lavine, A.S. (2011) Fundamentals of Heat and Mass Transfer, seventh ed., Wiley, New York.

Leonard, B.P. (1979) A stable and accurate convective modelling procedure based on quadratic upstream interpolation, Computer Methods in Applied Mechanics and Engineering 19, pp 59–98, DOI: 10.1016/0045-7825(79)90034-3

Li, Q., Yuan, X., Neveu, P., Flamant, G., Luo, L. (2014) A novel optimization approach to convective heat transfer enhancement for solar receiver, Chemical Engineering Science 16, pp 806–816, DOI: 10.1016/j.ces.2014.05.051

Li, Y., Liu, Z., Zheng, B. (2015) Experimental study on the saturated pool boiling heat transfer on nano-scale modification surface, International Journal of Heat and Mass Transfer 84, pp 550-561, DOI: http://dx.doi.org/10.1016/j.ijheatmasstransfer.2014.12.064

Liu, C., Wolfersdorf, J., Zhai, Y. (2015) Comparison of time-resolved heat transfer characteristics between laminar and turbulent with unsteady flow temperature, International Journal of Heat and Mass Transfer 84, pp 376-389, DOI: http://dx.doi.org/10.1016/ j.ijheatmasstransfer.2015.01.034

Liu, Y., Gehde, M. (2015) Evaluation of heat transfer coefficient between polymer and cavity wall for improving cooling and crystallinity results in injection molding simulation, Applied Thermal Engineering 80, pp 238-246, DOI: http://dx.doi.org/10.1016/j.applthermaleng. 2015.01.064

Mehrali, M., Sadeghinezhad, E., Rosen, M.A., Latibari, S.T., Metselaar, H.S.C. (2015) Effect of specific surface area on convective heat transfer of graphene nanoplatelet aqueous nanofluids, Experimental Thermal and Fluid Science, DOI: http://dx.doi.org/ 10.1016/ j.expthermflusci.2015.03.012

Meng, X., Yan, B., Gao, Y., Wang, J., Zhang, W., Long, E. (2015) Factors affecting the in situ measurement accuracy of the wall heat transfer coefficient using the heat flow meter method, Energy and Buildings 86, pp 754-765, DOI: http://dx.doi.org/10.1016/j.enbuild. 2014.11.005

Mirmanto, M. (2014) Heat transfer coefficient calculated using a linear pressure gradient assumption and measurement for flow boiling in microchannels, International Journal of Heat and Mass Transfer 79, pp 269-278, DOI: http://dx.doi.org/10.1016/ j.ijheatmasstransfer. 2014.08.022

Myers, R.H. (1976) Response Surface Methodology, first ed., Edwards Brother (Distributors), Virginia.

Oliveira, D.C., Almeida, C.A.K., Vieira, L.G.M., Damasceno, J.J.R., Barrozo, M.A.S. (2009) Influence of geometric dimensions on the performance of a filtering hydrocyclone: an experimental and CFD study, Brazilian Journal of Chemical Engineering 26, pp 575-583, DOI: http://dx.doi.org/10.1590/S0104-66322009000300013

Patankar, S.V., Spalding, D.B. (1972) A Calculation procedure for heat, mass and momentum transfer in three-dimensional parabolic flows, International Journal of Heat and Mass Transfer 15, pp 1787-1806, DOI: 10.1016/0017-9310(72)90054-3

Paul, T.C., Morshed, A.K.M.M., Fox, E.B., Khan, J.A. (2015) Experimental investigation of natural convection heat transfer of Al_2O_3 Nanoparticle Enhanced Ionic Liquids (NEILs), International Journal of Heat and Mass Transfer 83, pp 753-761, DOI: http://dx.doi.org/10.1016/j.ijheatmasstransfer.2014.12.067

Pitsch, H. (2006) Large-eddy simulation of turbulent combustion, Annual Review of Fluid Mechanics 38, pp 453–482, DOI: 10.1146/annurev.fluid.38.050304.092133

Silva, D.O., Vieira, L.G.M., Barrozo, M.A.S. (2015) Optimization of design and performance of solid-liquid separators: a thickener hydrocyclone, Chemical Engineering & Technology 38, pp 319-326, DOI: 10.1002/ceat.201300464

Sørum, M., Dorao, C.A. (2015) Experimental study of the heat coefficient deterioration density wave oscillations, Chemical Engineering Science, DOI: http://dx.doi.org/ 10.1016/j.ces.2015.03.039

Tavassoli, H., Peters, E.A.J.F., Kuipe, J.A.M. (2015) Direct numerical simulation of fluid–particle heat transfer in fixed random arrays of non-spherical particles, Chemical Engineering Science 16, pp 42–48, DOI:10.1016/j.ces.2015.02.024

Tzempelikos, D.A., Mitrakos, D., Vouros, A.P., Bardakas, A.V., Filios, A.E., Margaris, D.P. (2015) Numerical modeling of heat and mass transfer during convective drying of cylindrical quince slices, Journal of Food Engineering 156, pp 10-21, DOI: http://dx.doi.org/ 10.1016/j.jfoodeng.2015.01.017

Venkatachalapathy, S., Kumaresan, G., Suresh, S. (2015) Performance analysis of cylindrical heat pipe using nanofluids - An experimental study, International Journal of Multiphase Flow 72, pp 188-197, DOI: http://dx.doi.org/10.1016/ j.ijmultiphaseflow. 2015.02.006

Vieira, L.G.M., Barrozo, M.A.S. (2014) Effect of vortex finder diameter on the performance of a novel hydrocyclone separator, *Minerals Engineering* 57, pp 50-56, DOI: 10.1016/j.mineng.2013.11.014

Wallenstein, M., Kind, M., Dietrich, B. (2014) Radial two-phase thermal conductivity and wall heat transfer coefficient of ceramic sponges - Experimental results and correlation, International Journal of Heat and Mass Transfer 79, pp 486-495, DOI: http://dx.doi.org/ 10.1016/ j.ijheatmasstransfer. 2014.08.003

Whitaker, S. (1972) Forced convection heat transfer correlation for flow in pipes, past flat plates, single cylinders, single spheres and flow in packed beds and tube bundles, AIChE Journal 18, pp 361-371.

Xu, C., Yang, L., Li, L., Du, X. (2015) Experimental study on heat transfer performance improvement of wavy finned flat tuber, Applied Thermal Engineering, DOI: 10.1016/ j.applthermaleng.2015.02.024

Xu, J., Yang, C., Zhang, W., Sun, D. (2015) Turbulent convective heat transfer of CO_2 in a helical tube at near-critical pressure, International Journal of Heat and Mass Transfer 80, pp 749-758, DOI: http://dx.doi.org/10.1016/ j.ijheatmasstransfer.2014.09.066

Zhao, T., Liu, K., Murata, H., Harumi, K., Takei, M. (2015) Investigation of bed-to-wall heat transfer characteristics in a rolling circulating fluidized bed, Powder Technology 269, pp 46-54, DOI: http://dx.doi.org/10.1016/j.powtec.2014.08.068

Zhukauskas, A. (1972) Heat Transfer from tubes in cross flow, Advances in Heat Transfer 8 Academic Press, New York.

****